Design and demonstration of a colorless WDM-OFDMA PON system architecture achieving symmetric 20-Gb/s transmissions with residual interference compensation

Hsing-Yu Chen,[1,2,*] Maria Yuang,[3] Po-Lung Tien,[4] Dar-Zu Hsu,[2] Chia-Chien Wei,[5] Yu-Shen Tsai,[1] and Jyehong Chen[1]

[1] *Department of Photonics, National Chiao-Tung University, Hsinchu, Taiwan, 300*
[2] *Information and Communications Research Labs, Industrial Technology Research Institute, Hsinchu, Taiwan, 300*
[3] *Departments of Computer Science, National Chiao-Tung University, Hsinchu, Taiwan, 300*
[4] *Departments of Electrical Engineering, National Chiao-Tung University, Hsinchu, Taiwan, 300*
[5] *Department of Photonics, National Sun Yat-sen University, Kaohsiung, Taiwan, 300*
**starchen@itri.org.tw*

Abstract: In this paper, we propose a two-tiered colorless WDM-OFDMA PON system architecture that draws strengths from each individual WDM and OFDM PON systems. Specifically, the two-tiered architecture enables a colorless transceiver to be shared by a group of ONUs, resulting in drastic reduction of the system cost. For achieving colorlessness via reusing downstream light sources, we discover the residual power of downstream signal unexpectedly springs back after transmissions, causing severe interference to the upstream signal, and thus limiting the data rate of the upstream signal. We devise a method of adopting a common dispersion compensation module at OLT to reduce the residual power over all wavelengths. Experimental results show that, with an improvement of upstream signal's SNR up to 10dB, the system successfully achieves 20-Gb/s bidirectional OFDM-signal transmissions on the same wavelength over a 20-km SMF.

OCIS codes: (060.2330) Fiber optics communications; (060.4080) Modulation.

References and links

1. Y.-M. Lin and P.-L. Tien, "Next-generation OFDMA-based passive optical network architecture supporting radio-over-fiber," IEEE J. Sel. Areas Comm. **28**(6), 791–799 (2010).
2. D. Qian, N. Cvijetic, J. Hu, and T. Wang, "A novel OFDMA-PON architecture with source-free ONUs for next-generation optical access networks," IEEE Photon. Technol. Lett. **21**(17), 1265–1267 (2009).
3. C. Hsing-Yu, W. Chia-Chien, H. Dar-Zu, M. C. Yuang, C. Jyehong, L. Yu-Min, T. Po-Lung, S. S. W. Lee, L. Shih-Hsuan, L. Wei-Yuan, H. Chih-Hung, and S. Ju-Lin, "A 40-Gb/s OFDM PON System Based on 10-GHz EAM and 10-GHz Direct-Detection PIN," IEEE Photon. Technol. Lett. **24**(1), 85–87 (2012).
4. J. H. Lee, K.-M. Choi, J.-H. Moon, and C.-H. Lee, "Seamless upgrades from a TDM-PON with a video overlay to a WDM-PON," J. Lightwave Technol. **27**(15), 3116–3123 (2009).
5. S.-G. Mun, H.-S. Cho, and C.-H. Lee, "A Cost-Effective WDM-PON Using a Multiple Section Fabry–Pérot Laser Diode," IEEE Photon. Technol. Lett. **23**, 3–5 (2011).
6. M. C. Yuang, P.-L. Tien, D.-Z. Hsu, S.-Y. Chen, C.-C. Wei, J.-L. Shih, and J. Chen, "A high-performance OFDMA PON system architecture and medium access control," J. Lightwave Technol. **30**(11), 1685–1693 (2012).
7. D.-Z. Hsu, C.-C. Wei, H.-Y. Chen, W.-Y. Li, and J. Chen, "Cost-effective 33-Gbps intensity modulation direct detection multi-band OFDM LR-PON system employing a 10-GHz-based transceiver," Opt. Express **19**(18), 17546–17556 (2011).
8. B. Liu, X. Xin, L. Zhang, J. Yu, Q. Zhang, and C. Yu, "A WDM-OFDM-PON architecture with centralized lightwave and PolSK-modulated multicast overlay," Opt. Express **18**(3), 2137–2143 (2010).

#193159 - $15.00 USD Received 1 Jul 2013; revised 2 Aug 2013; accepted 11 Aug 2013; published 3 Sep 2013

9. J. L. Wei, E. Hugues-Salas, R. P. Giddings, X. Q. Jin, X. Zheng, S. Mansoor, and J. M. Tang, "Wavelength reused bidirectional transmission of adaptively modulated optical OFDM signals in WDM-PONs incorporating SOA and RSOA intensity modulators," Opt. Express **18**(10), 9791–9808 (2010).
10. J. Yu, M.-F. Huang, D. Qian, L. Chen, and G.-K. Chang, "Centralized lightwave WDM-PON employing 16-QAM intensity modulated OFDM downstream and OOK modulated upstream signals," IEEE Photon. Technol. Lett. **20**(18), 1545–1547 (2008).
11. L. Gong-Ru, L. Yi-Hung, L. Chun-Ju, C. Yu-Chieh, and L. Gong-Cheng, "Reusing a Data-Erased ASE Carrier in a Weak-Resonant-Cavity Laser Diode for Noise-Suppressed Error-Free Transmission," IEEE J. Quantum Electron. **47**(5), 676–685 (2011).
12. K. Hoon, K. Sangho, H. Seongtaek, and O. Yunje, "Impact of dispersion, PMD, and PDL on the performance of spectrum-sliced incoherent light sources using gain-saturated semiconductor optical amplifiers," J. Lightwave Technol. **24**(2), 775–785 (2006).
13. A. D. McCoy, P. Horak, B. C. Thomsen, M. Ibsen, and D. J. Richardson, "Noise suppression of incoherent light using a gain-saturated SOA: implications for spectrum-sliced WDM systems," J. Lightwave Technol. **23**(8), 2399–2409 (2005).
14. S. H. Cho, S. S. Lee, and D. W. Shin, "Transmission performance enhancement for EIN limited 2.5 Gbit/s RSOA-based WDM-PON by using dispersion management," Electron. Lett. **46**(9), 636–638 (2010).

1. Introduction

Orthogonal frequency-division multiple access (OFDMA) [1–3] and wavelength division multiplexing (WDM) [4, 5] PONs have been envisioned as prominent technologies for next-generation passive optical networks (PONs). OFDMA PON offers high spectral efficiency and flexible sub-channel bandwidth allocation. However, the optical beat interference (OBI) problem results in the severe degradation of signal performance. In our previous work [6], we have designed a virtual-tree OFDMA PON system (VTOPS) architecture and demonstrated that the OBI problem has been successfully eliminated due to the virtual tree architecture. To improve the spectral efficiency, OFDM PON typically employs high-order quadrature amplitude modulation (QAM), which requires a high signal-to-noise ratio (SNR). As a result, the number of optical network units (ONUs) that can be connected to optical line terminal (OLT) is severely limited.

Contrastingly, for a WDM PON system, it is simpler to support more ONUs merely by adding wavelengths. However, the available enhancement bands provide limited bandwidth at C-band for future PONs that are expected to coexist with current PONs [7], thus limiting the allowable number of wavelengths in WDM systems. Besides, the need for temperature controllers for WDM lasers at each ONU drastically increases the overall cost of WDM PON systems. As a result, the colorless/wavelength-reusable WDM systems [8–10] have been devised as an efficient way of reducing the number of wavelengths. Specifically, a colorless WDM PON system allows any light source from OLT for carrying downstream signals to be re-used via colorless transceivers (CLTs) at ONUs to transport upstream signals. The CLTs are implemented by devices, such as Mach-Zehnder modulator (MZM) [8, 10], or reflective semiconductor optical amplifier (RSOA) [9], which are currently expensive. This fact makes colorless WDM PON systems uneconomical when supporting a large number of ONUs. Furthermore, for reusing downstream light sources by employing gain saturated SOA, we discover that the residual power of downstream signal unexpectedly springs back after transmissions, causing severe interference and performance degradation to the upstream signal [11–14]. As a result, these colorless systems [8, 10] can only support limited data rates for upstream transmissions.

In this paper, we propose a two-tiered colorless WDM-OFDMA PON system architecture that draws strengths from each individual WDM and OFDM PON systems, while overcoming their weaknesses described above. Specifically, the two-tiered architecture enables a CLT to be shared by a group of ONUs, resulting in drastic reduction of the system cost. Furthermore, to reduce the residual power of downstream signals after the CLT, we adopted a common dispersion compensation module at OLT over all wavelengths. Experimental results show that, with an improvement of upstream signal's SNR at the highest frequency up to 10dB, the

#193159 - $15.00 USD Received 1 Jul 2013; revised 2 Aug 2013; accepted 11 Aug 2013; published 3 Sep 2013

system successfully achieves 20-Gb/s bidirectional OFDM-signal transmissions on the same wavelength over a 20-km SMF.

2. System architecture

As shown in Fig. 1, the colorless WDM-OFDMA PON is a two-tiered system, which connects a total of $W \times N$ ONUs to OLT, where W is the total number of wavelengths, and N is the number of ONUs in a *section* sharing the same wavelength. Notice that, each section corresponds to a geographic area within the PON. In the first tier, the OLT is directly connected to W sections of ONUs through a WDM multiplexer (i.e., array waveguide grating (AWG)), a WDM AWG demultiplexer, and W short trunk fibers. In this tier, the tree structure is exhibited and the transmission is on wavelength basis. In the second tier, each WDM AWG demultiplexer port is further connected to a section containing N ONUs through an optical distribution node (ODN). In this tier, a virtual-tree structure [6] is employed, and the transmission is on OFDM basis.

In each section, its ODN is composed of a power splitter, N three-port bypassable circulators (each of which connects to an ONU), and a colorless transceiver (CLT). To satisfy the colorlessness requirement, the power splitter of a section in ODN distributes the downstream OFDM signal to two optical beams. The first optical beam from the power splitter is passed to ONU1 of the section for node-by-node downstream receptions and upstream transmissions. The second optical beam from the power splitter is directed to the CLT for being reused as a light source for the colorless upstream transmissions of the entire section.

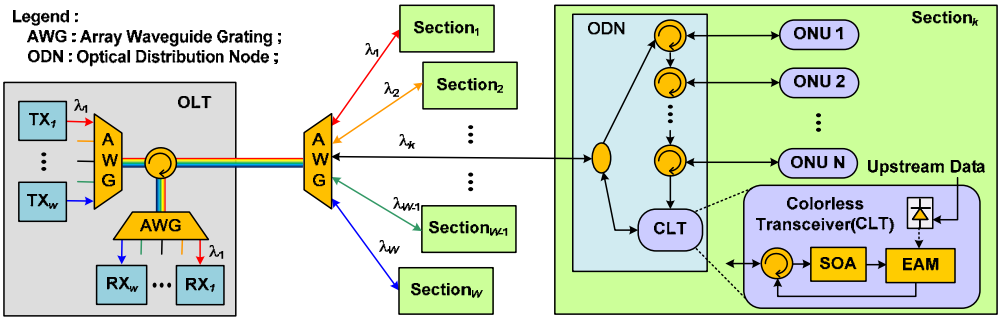

Fig. 1. Architecture of the two-tiered colorless WDM-OFDMA PON system.

At each ONU, the downstream OFDM signal is received by the optical receiver and converted into its electrical form. If the destination address matches with that of the ONU, the data are dropped, and then the ONU inserts its upstream data using the determined subcarriers of the OFDM signal. Together with the remaining downstream data, the combined OFDMA signal is modulated and optically transmitted to the next ONU. Because the signal is regenerated at every ONU, the optical power budget is only needed to cover the optical link loss from OLT to the first ONU or from the CLT to OLT, while the first ONU can be managed to remain always-on [6].

The CLT for each section is shared by all ONUs in the same section, thus reducing the system cost. As shown in Fig. 1, the CLT for a section consists of a photodiode, an electro-absorption modulator (EAM), a nonlinear SOA, and a circulator. The photodiode is used to receive the aggregated upstream OFDM signal from the last ONU in the section. Recall that the second optical beam from the power splitter is directed to the CLT. This beam is first passed to the nonlinear SOA, operating in the saturation region in order to erase the unwanted downstream OFDM signals. The EAM then uses this light source to modulate the aggregated upstream data received by the photodiode. Finally, the upstream signal is passed from EAM

#193159 - $15.00 USD Received 1 Jul 2013; revised 2 Aug 2013; accepted 11 Aug 2013; published 3 Sep 2013

through the circulator, then the splitter of this section, and ultimately to the OLT via the same (downstream) fiber trunk.

3. Experimental setup and results

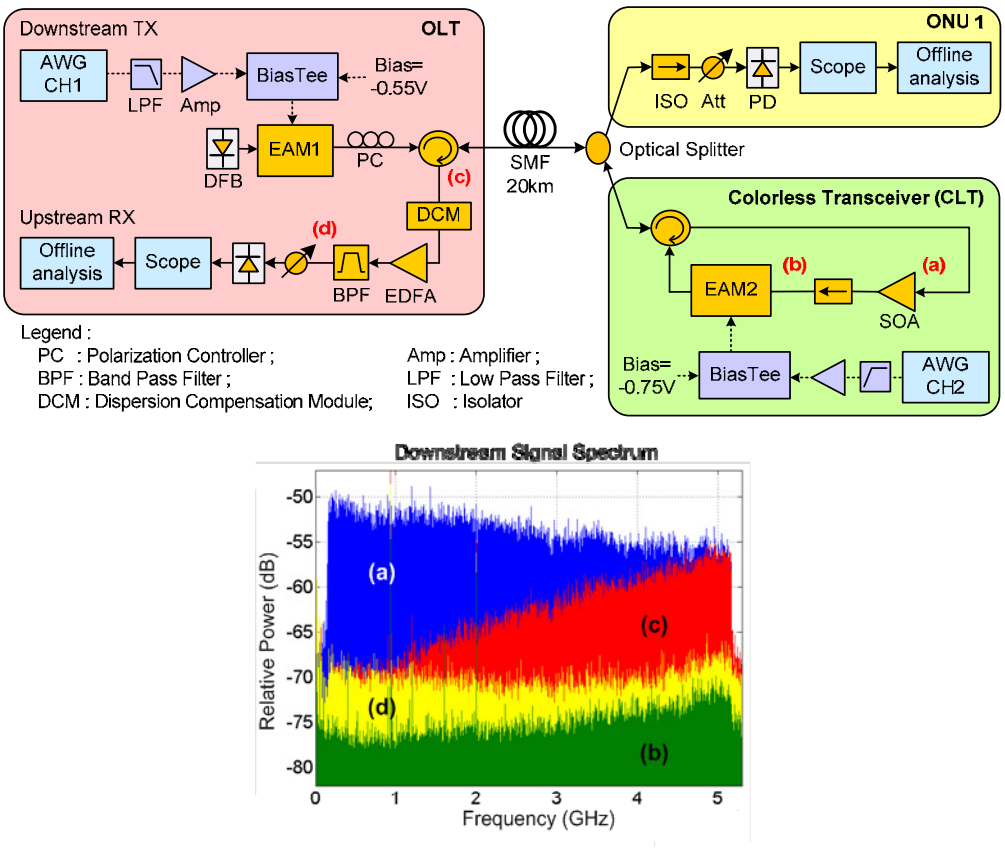

Fig. 2. Experimental setup of point-to-point downstream and upstream transmission, and the spectra of the downstream signals (a) before the SOA, (b) after the SOA, (c) after a 20-km SMF transmission, and (d) after the DCM and the pre-amplifier.

The experimental setup is shown in Fig. 2. In the experiment, we employ two representative point-to-point transmissions: downstream from OLT to ONU1, and upstream from CLT to OLT. Both downstream and upstream OFDM signals are generated by an arbitrary waveform generator (AWG, Tektronix® AWG7122) using Matlab®. The OFDM transmitter consists of serial-to-parallel conversion, (QAM) modulation, inverse fast Fourier transform (IFFT), cyclic prefix (CP) insertion, and digital-to-analog conversion (DAC). The sampling rate and DAC resolution of the AWG are 12-GS/s and 8 bits, respectively. Both the downstream and upstream driving signals consist of 16-QAM OFDM signals with an FFT size of 512, CP of 8, and the data are encoded at 7th ~220th subcarriers with the total bandwidth of 5 GHz, yielding the symmetric raw data rates of 20-Gb/s. The downstream optical signal is generated by a 10-GHz EAM1 biased at –0.55V. After passing through a 20-km SMF, a power splitter splits the power equally to ONU1 and CLT. In ONU1, the downstream signal is detected by a 10-GHz PIN receiver, while the electrical signal is captured by a digital oscilloscope (Tektronix® DPO 71254) with 50-GS/s sampling rate and 3-dB bandwidth of 12.5-GHz. The digitized signal is demodulated and analyzed by Matlab® with 1/10 training symbols. At

#193159 - $15.00 USD Received 1 Jul 2013; revised 2 Aug 2013; accepted 11 Aug 2013; published 3 Sep 2013

CLT, the received downstream signal is first amplified and erased by a saturated SOA, then modulated by a 10-GHz EAM2 to generate the upstream signal.

Crucially, since a saturated SOA can only remove intensity modulation of downstream signal, the residual and SOA-induced phase modulation is converted back to intensity modulation following dispersive transmissions. Such a spring back of the earlier erased OFDM signal severely degrades the upstream OFDM signal quality after transmission. To resolve this issue, we exploit a DCM (that can be replaced by a common DCF), which is a chirped FBG, to suppress the sprung residual downstream signal, while having the upstream OFDM signal received by a 10-GHz PIN receiver with an EDFA and a band pass filter to remove the out-of-band ASE noise. Notice that the overall system cost remains low due to the fact that both the DCM and pre-amplifier are shared by all wavelength sections. In Fig. 2, we illustrate the electrical spectra of the downstream signal taken at different points. The downstream spectrum after a 20-km transmission is shown by curve (a). The subcarrier power that is suppressed via a nonlinear saturated SOA with −13dBm injected power by 20~25 dB is shown in curve (b). Curve (c) depicts how chromatic dispersion causes the residual downstream power to spring back after fiber transmission. Notice that, because dispersion induces a greater phase shift for higher-frequency components, we observe relatively greater spring back at higher frequencies. Finally, the spectrum of the residual downstream signal after the DCM (see curve (d)) indicates that the residual power can be effectively suppressed when compared with curve (c). Furthermore, we show the optical spectra of the optical carrier without and with modulation (at both the input and output of the SOA) in Figs. 3(a) and 3(b),

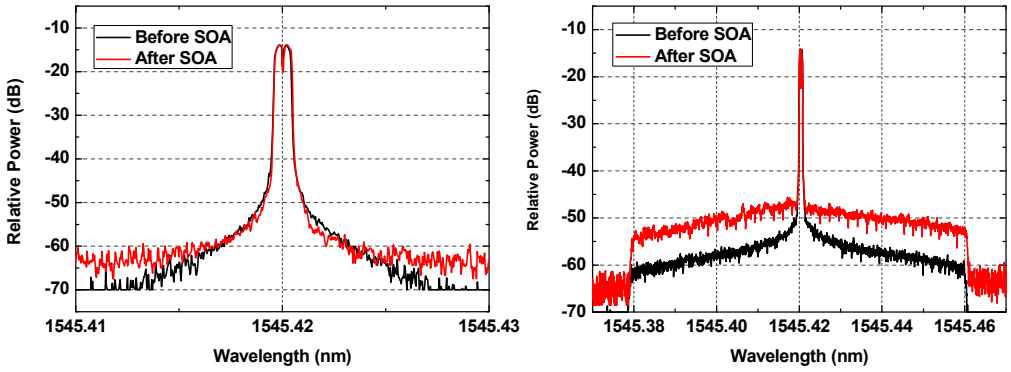

Fig. 3. The optical spectra of (a) the optical carrier without modulation, and (b) the modulated optical carrier, before and after the SOA.

respectively. The spectrum of the coherent light source is not expanded after passing through the SOA, which is different from that of the incoherent light source using the spectrum slicing method [12–14].

Furthermore, we show in Fig. 4 the SNR performance under five downstream/upstream cases (Figs. 4(a) and 4(b)) and one additional upstream case (Fig. 4(b)). The first case corresponds to an optical back-to-back (B-t-B) transmission, as shown by curves “B-t-B” for the downstream and upstream transmissions, respectively. The B-t-B case can be treated as the best-case scenario, which is free from Rayleigh backscattering and residual downstream signal interference. In the second case, the upstream and downstream data are carried via different fibers. Almost no SNR penalty is exhibited by the two “d-fiber”curves in Fig. 4. In the third case, the downstream and upstream signals are together transmitted via the same fiber (see “s_fiber” curves), but only with the downstream or upstream data encoded and the other flow replaced by a CW signal. In this case, Rayleigh backscattering causes SNR degradation. Due to higher launch upstream power than downstream power, the SNR degradation for the downstream signal is more severe than that for the upstream signal.

#193159 - $15.00 USD Received 1 Jul 2013; revised 2 Aug 2013; accepted 11 Aug 2013; published 3 Sep 2013

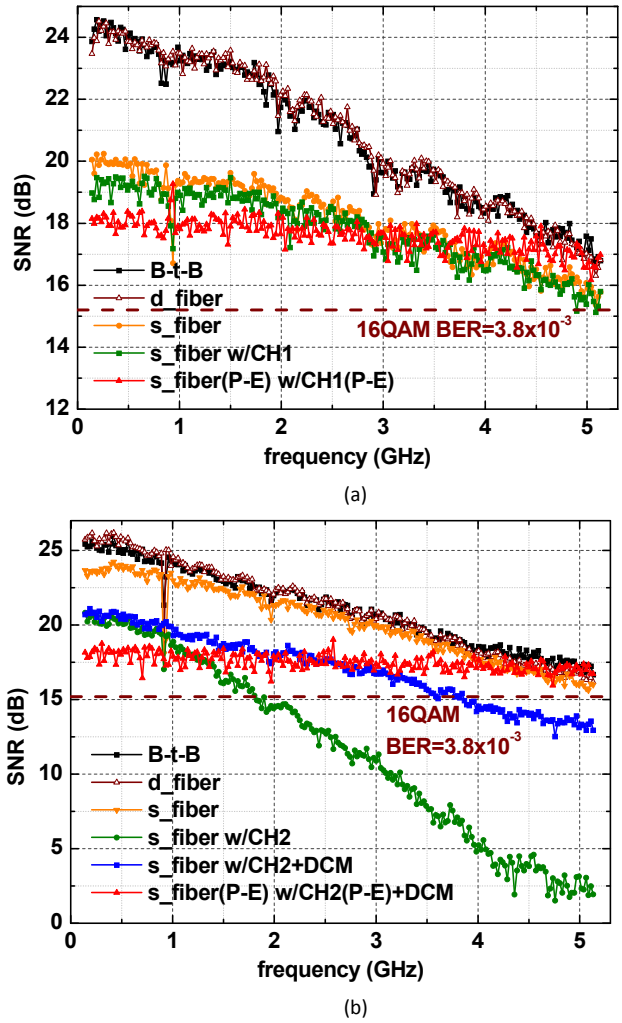

Fig. 4. SNR performances of (a) the downstream signal, and (b) the upstream signal.

#193159 - $15.00 USD Received 1 Jul 2013; revised 2 Aug 2013; accepted 11 Aug 2013; published 3 Sep 2013

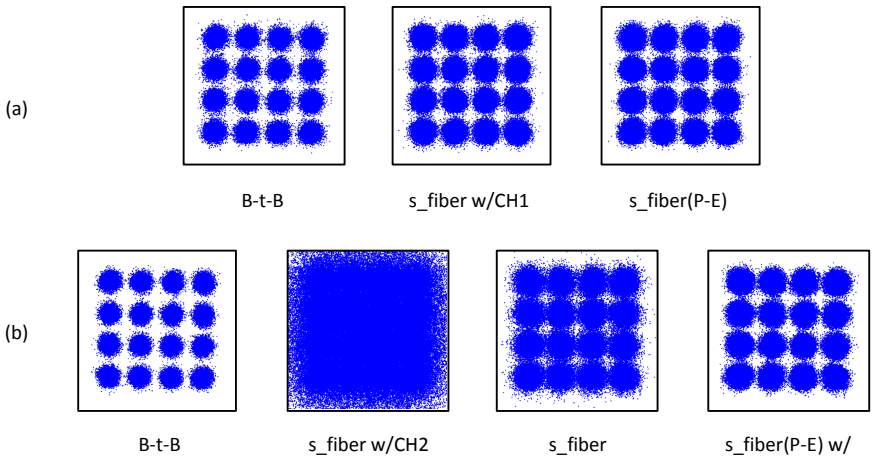

Fig. 5. Constellations of the (a) downstream signal, and (b) upstream signal, corresponding to the cases in Fig. 4, at the received power of −12 dBm.

In the fourth case, both upstream and downstream data are encoded and carried via the same fiber, as shown by the curves "s_fiber w/CH1" and "s_fiber w/CH2" for downstream and upstream, respectively. We clearly observe severe degradation of the upstream signal performance, resulted from the spring back of the residual downstream signal. In the fifth case, significantly, after applying the DCM method, the residual interference is suppressed, as shown in curve "s_fiber w/CH2+DCM" of Fig. 4(b). The method yields an improvement of the SNR at high frequencies by up to 10 dB. We next illustrate in Fig. 5 the corresponding constellations of several cases in Fig. 4. Here, the improvement in signal quality provided by the DCM can also be clearly observed from the constellations. For the final case, we apply power pre-emphasis to equalize the SNR across all subcarriers. After applying power pre-emphasis, as shown in Fig. 4, we obtain smoother SNR curves (see curves "s_fiber(P-E) w/CH1(P-E)" and "s_fiber(P-E) w/CH2(P-E)+DCM").

Finally, we illustrate in Fig. 6 the BER of the 20-Gb/s downstream and upstream signals after a 20-km bidirectional SMF transmission. The results demonstrate that a BER of less than 3.8×10^{-3} (FEC threshold) can be attained for downstream and upstream signals with the received powers of −15 dBm and −15.8 dBm, respectively.

#193159 - $15.00 USD Received 1 Jul 2013; revised 2 Aug 2013; accepted 11 Aug 2013; published 3 Sep 2013

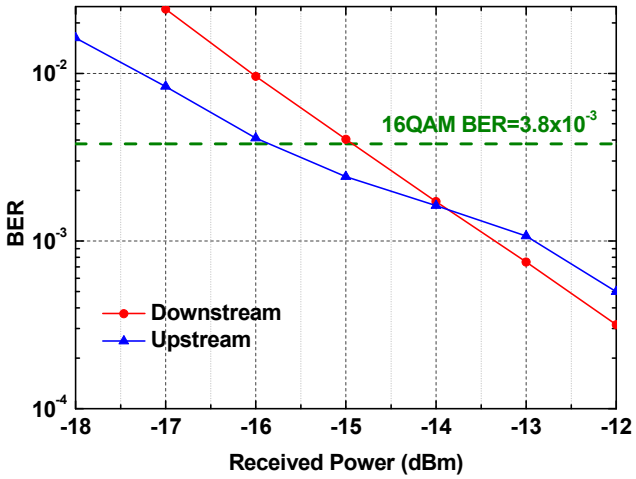

Fig. 6. The BER curve of the downstream and upstream OFDM signals after a 20-km fiber transmission.

5. Conclusions

We have proposed a new two-tiered colorless WDM-OFDM PON system architecture. The architecture is not only free from the OBI problem but also allows each colorless transceiver to be economically shared by a group of ONUs. Significantly, the system is augmented with a residual interference compensation technology when applying the re-use of light sources. We have conducted an experiment to investigate the impact of the spring back of the residual downstream OFDM signal on the performance of the upstream OFDM signal. We then justify that, by applying the residual interference compensation, namely the DCM method, we could effectively suppress the signal interference, and improve the SNR at the highest frequency of the upstream signal by up to 10 dB. Finally, experimental results demonstrate that the system successfully achieves 20-Gb/s downstream and upstream OFDM-signal transmissions simultaneously on the same wavelength over the same 20-km SMF.

#193159 - $15.00 USD Received 1 Jul 2013; revised 2 Aug 2013; accepted 11 Aug 2013; published 3 Sep 2013